

Comparison of Dinitrogen, Methane, Carbon Monoxide, and Carbon Dioxide Mass-Transport Dynamics in Carbon and Zeolite Molecular Sieves

by György Onyestyák

Institute of Nanochemistry and Catalysis, Chemical Research Center, Hungarian Academy of Sciences,
Pusztaszeri út 59–67, H-1025 Budapest
(phone: +36-1438-1100; fax: +36-1-438-1143; e-mail. ony@chemres.hu)

Equilibrium (based on *Henry* constants) and kinetic (based on relaxation-time constants or rather macropore transport diffusivities) selectivities for commercial zeolite and carbon-molecular-sieve (CMS) adsorbents were compared. Adsorption isotherms were recorded at -20° . The frequency-response (FR) sorption-rate spectra were determined in the range of -78 and 70° at 133 Pa. In particles of a larger size than 1.0 mm, macropore diffusion governed the rate of sorption mass transport in both types of microporous materials. The differences in the intercrystalline diffusivities established the kinetic separation of the gases notwithstanding the essential importance of interactions in the micropores. Zeolites seem to be more advantageous for a dynamic separation of CO_2 and CH_4 than CMS 4A. With the CO_2 and CO pair, the CMS is characterized by short characteristic times which, together with a good separation factor, is a double advantage in a short-cycle adsorption technology. Upon comminution of the carbon pellets, intercrystalline-diffusion resistance can be completely removed by using CMS 4A adsorbent particles with a diameter smaller than 1 mm. The carbonization of spruce-wood cubes resulted in an excellent carbon honeycomb structure, which seems to be ideal from a dynamic point of view for applications in short-cycle adsorption-separation technologies. In the development of adsorbents, the use of the FR method can be beneficial.

Introduction. – Microporous solids, such as zeolites and activated carbons are widely used in gas-separation processes. Separation is based on the selectivity of the adsorbent for the adsorption of different gas molecules. In equilibrium, the selectivity can reflect the differences in the adsorption energies of the gas components. The adsorption selectivity is greatly enhanced if molecular sieving is effective [1]. Independent from the equilibrium selectivity, transient adsorption selectivity appears during equilibration if the sorption dynamics of the gas components are different. Short-cycle adsorption-separation technologies, such as pressure-swing adsorption (PSA), have been applied to many separation and purification operations in a range of industries [2]. The favorable PSA adsorbents have high adsorption selectivity and capacity. It is important that adsorption/desorption should rapidly follow the applied periodic pressure change. Up to now, very few frequency-response (FR) ‘rate-spectroscopic’ studies have been devoted to the dynamics of sorption systems having commercial importance [3][4].

Dinitrogen, methane, carbon monoxide and carbon dioxide are important in many industrial applications, as well as in our daily life. The increasing concentration of CO_2 in the atmosphere furnishes a major contribution to the global warming. Separation of CO_2 from mostly N_2 -containing stack gases is important from this aspect [5].

Separation of CH₄ and CO₂ is wanted for recovering CH₄ from landfill gas and also to upgrade natural gas [6]. Separation of CO/CO₂ mixtures has also industrial significance, because CO is a valuable raw material for the synthesis of a large variety of chemicals; however, CO-selective adsorbents are available to only a very limited extent [7].

Improvements in performance and the reduction in cost of adsorption processes are dependent on parameters which are dictated by adsorbent loading per unit volume, mass-transfer properties, pressure drop, and thermal management. However, these factors are strongly influenced by the structure of the adsorbent used in the gas-separation device. A major driver toward the development of future adsorptive gas-separation processes lies in the development of improved sorbent materials [8]. A key area of future research is the mass-transfer characteristics. The influence of adsorbent structure on mass-transport kinetics influences the overall system efficiency. The relationship between separation performance and the macro/meso/micro hierarchy of the adsorbent has not been explored to date. Pore engineering must be integrated with systems engineering to produce an overall optimal structure.

In the present study, the dynamic adsorption properties of different zeolite and carbon adsorbents are compared taking advantage of the unique potentials of the FR method [9]. It is a transient method wherein the equilibrium of a gas/solid system is periodically perturbed at varying frequencies, while a response function is recorded. In the batch-type FR unit used in the present work, the volume of the sorption chamber was modulated, and a response pressure wave was recorded. Resonance is observed if the perturbation and a transport process occur on the same time scale. Plotting the real and the imaginary part of the complex response function in function of the modulation frequency is a convenient way of displaying the results. The frequency value at which the imaginary function goes through a maximum is related to the mass-transport time constant for the adsorbate/adsorbent system at the pressure and temperature of the experiment. The known batch FR units working at low pressure, *i.e.*, low coverage (where the slope of adsorption isotherms obtained on microporous materials is high resulting in high sensitivity), are not suitable to simulate directly the high-pressure commercial PSA units. However, meaningful FR results could be obtained by applying $\pm 1\%$ pressure variation at a mean of 133 Pa, which can advance development of adsorbents.

Experimental. – *Materials.* The adsorption properties of synthetic 4A (MS514), 5A (SP7-9253.01), and 13X (C544) zeolite beads, obtained from *Grace GmbH*, and carbon molecular sieve, CMS 4A (MSC-4A) pellets, manufactured by *Takeda Chemical Co.*, were compared. The adsorbent particles (zeolite beads and cylindrical carbon pellets) had about the same diameter (*ca.* 2.1 mm). Besides the MSC-4A extrudates, other carbon samples were also characterized such as *i*) commercial activated-carbon (AC) pellets (WS IV.) of 3.0 mm diameter obtained from *Chemviron* and *ii*) charcoal samples made from wood in our laboratory. The latter samples were prepared from cubes (1 × 1 × 1 cm), cut from a Norway spruce log, by a single-step carbonization in a N₂ flow at 700° for 60 min. The obtained material had molecular-sieve properties (CMS cubes) [10]. A second sample was prepared from the CMS cubes by steam activation (900°, 15 min), followed by HNO₃ treatment (AC cubes). The cubes were kept immersed in 1M HNO₃ soln. at r.t. for 6 d. The pellets were crushed and sieved to different-particle-size fractions to get samples of particles having different diffusion-path lengths.

Methods. N₂ Adsorption isotherms were measured at –196° with a *Quantachrome-Autosorb1C* apparatus. Analysis giving morphology data was performed by the *Quantachrome* software. An all-glass

manometric system and batch-type FR system [11] was used to determine N₂, CH₄, CO, and CO₂ adsorption isotherms at –20° and sorption-rate spectra, resp. The FR rate spectra were determined in the 0.001–10 Hz frequency range between –78, 0, 20, 30, and 70° and at 133 Pa. The –20° and –78° temperatures were maintained by using a bath of NaCl/granulated ice and dry ice, resp. Before adding adsorbates (high purity N₂, CH₄, CO, or CO₂), the samples were pretreated by a 3 h evacuation at 350°/10^{–5} Pa. Relaxation time constants and transport diffusivities were determined from theoretical FR functions showing the best fit to the experimental FR data [11][12].

The scanning-electron-microscope images were taken by a *Hitachi-S-570* SEM apparatus.

Results and Discussion. – If adsorption equilibrium is approached more rapidly by one of the gas components than by the others, its concentration will decrease most rapidly in the gas phase. An adsorption technology can be established for the separation of the components of significantly different sorption rates. For example, CMS materials are very often used for N₂ production from air because of the faster penetration of the slightly smaller O₂ molecules into the micropores. Molecular-sieve materials, zeolites, and carbon molecular sieves can distinguish and selectively adsorb molecules having the size and shape which permits them to enter the micropores. However, the real simple sieving effect is quite a curio. It is essential to learn more about the mass-transport kinetics of sorption. The potentials of the frequency-response (FR) method were exploited to reach this goal.

The in-phase (□) /real/ and the out-of-phase (○) /imaginary/ components of the complex response function are plotted against the modulation frequency to get the FR spectra (see *Fig. 1*). The plots show a step in the in-phase and a peak in the out-of-phase spectral component at the frequency of the resonance. A unique feature of the FR technique is that, for simple systems, conclusions can be drawn about the mechanism of the rate-governing transport process from the shape of the spectrum. In *Fig. 1*, the data points can be fitted well with simple theoretically derived FR spectra, usually referred as characteristic curves [13]. The single resonance suggests that only one process step controls the rate of sorption. The imaginary and real components of the complex response function approached each other asymptotically at high frequencies. Theoretically, such a spectrum is expected when pure diffusional mass transport is the slowest, rate-controlling step of sorption. According to *Fig. 1*, in pellets of zeolite 13X as well as CMS 4A, diffusion governs the rate of sorption. Surprisingly, the corresponding FR spectra of pelletized zeolite Na-X and CMS 4A particles of the same size are similar. The diffusion coefficients in the crushed- and sieved-zeolite-particle fractions were found to be independent on particle dimensions in a wide range suggesting that the rate-controlling diffusion proceeds within the intercrystalline macro- and mesopores. The N₂-rate spectra recorded on the CMS 4A and zeolite 13X pellets (the resonance frequencies and the intensities of the signals/reflecting the sorption capacities) were found to be virtually the same. This suggests that, regarding the rate-determining macropore diffusion, the structural differences in the nanometer range of pellets are irrelevant. In CMS 4A, the diffusion rates of N₂ and CO (having similar molecular mass and size) are hardly different; consequently, it is not feasible to use the adsorbent CMS 4A for the separation of these gases. Regarding N₂ and CH₄ separation, 13X does not show kinetic selectivity, while the kinetic selectivity of CMS 4A ($D_{N_2}/D_{CH_4} = t_{CH_4}/t_{N_2} = 10$, see *Table 3*, below) is significant. CH₄ has a stronger interaction with the carbon than N₂. The stronger interaction with the surface results in higher coverage and a

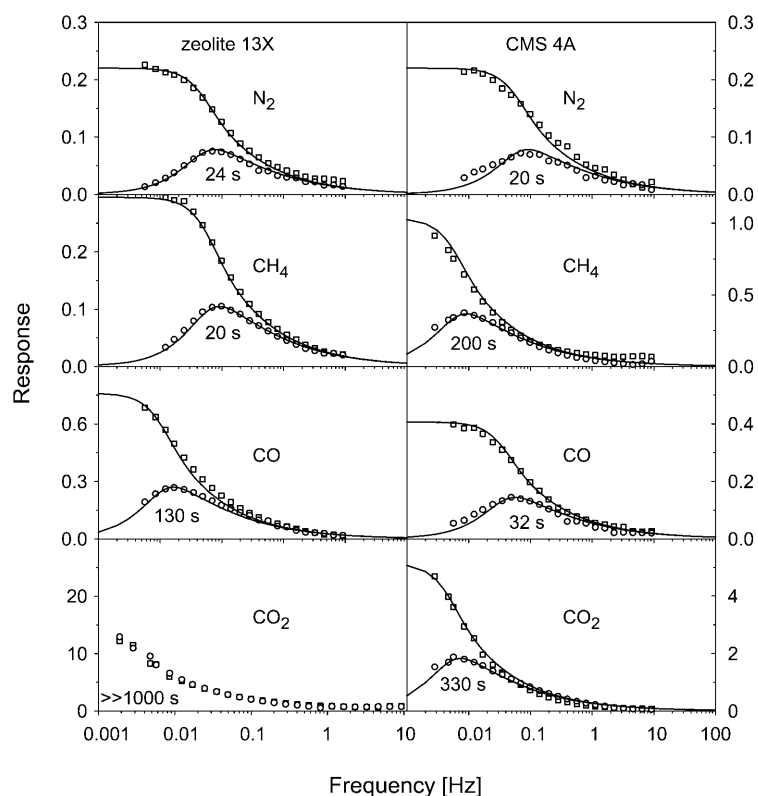


Fig. 1. FR Spectra of N_2 , CH_4 , CO , and CO_2 obtained in zeolite 13X beads and in CMS 4A pellets (ca. 500 mg samples) at 133 Pa and -20° . The samples were activated by a 3 h evacuation at 350° . The 133 Pa pressure was modulated at each frequency by $\pm 1\%$. Symbols represent measured data points corresponding to 'in-phase' (\square) and 'out-of-phase' (\circ) components of experimentally determined response functions. The line gives the best-fit theoretical function. Diffusion-time constants are given at the peaks.

slower diffusion inside the pellets. The differences in the intercrystalline diffusivities establish the kinetic separation of the gases.

The micropores are wider in zeolite 13X than in CMS 4A (see Table 1), whereas zeolite crystals, forming the 13X beads, are much larger (ca. $1\ \mu\text{m}$) than the graphitized domains of the carbons (a few nm). The longer intracrystalline diffusion path in the larger NaX crystallites can compensate the faster diffusivity in its wider micropores resulting in similar values of diffusion-time constants for the two adsorbents, *i.e.*, very similar FR spectra. The size of the micropores of zeolite 4A and CMS 4A is commensurable. The sorption transport of the N_2 , CH_4 , and CO_2 molecules seem to be too slow in the zeolite pores to get resonance signal within the available frequency window. For CO sorption, the asymptotic approach of the characteristic functions at higher frequencies as well as the nearly identical diffusion-time constant obtained for both the bead and the powdered form zeolite 4A suggests that intracrystalline diffusion

Table 1. Morphology Data of the Samples Obtained from N_2 Isotherms at -196°

	V_{total} [cm^3/g] ^{a)}	V_{micro} [cm^3/g] ^{b)}	S [m^2/g] ^{c)}	w [nm] ^{d)}
Zeolite 5A	0.32	0.26	705	0.45
Zeolite 13X	0.36	0.29	802	0.78
CMS-4A Pellet	0.20	0.17	490	0.49
AC Pellet	0.75	0.64	1570	1.25
CMS Cube	0.20	0.19	457	0.43
AC Cube	0.19	0.17	366	1.17

a) V_{total} = total pore volume at $p/p_0 = 0.95$. b) V_{micro} = micropore volume. c) S = specific surface area. d) w = average width of the micropores.

is the rate-governing step of CO sorption in zeolite 4A. The low resonance frequencies reflect slow mass transport, consequently zeolite 4A should not be used in rapid-cycle CO separation from gas mixtures.

In contrast to zeolite 4A, the CMS 4A powder can more rapidly adsorb the studied gases, including CO_2 (Fig. 2). The resonance frequency corresponds to a diffusion-time constant, r^2/D , where D is the diffusion coefficient and r is the particle radius. It should be noted that the microporous graphitized domains in carbon are much smaller than in the zeolite 4A crystals, *i.e.*, the length of the diffusion path in graphite domains is much shorter than in the zeolite crystals. An outstanding advantage of the FR method is its ability to study diffusion in an anisotropic system distinguishing different molecular mobilities, *e.g.*, two independent intracrystalline-diffusion processes. The multiple FR spectrum of CO_2 sorption in powdered CMS 4A suggests that parallel sorption processes proceed with different time constants. Similar spectra having two resonance signals were obtained earlier with NH_3 , propane, and CO_2 on activated carbon [9][14]. The different FR spectra of the pellets and ground CMS 4A demonstrate different rate-

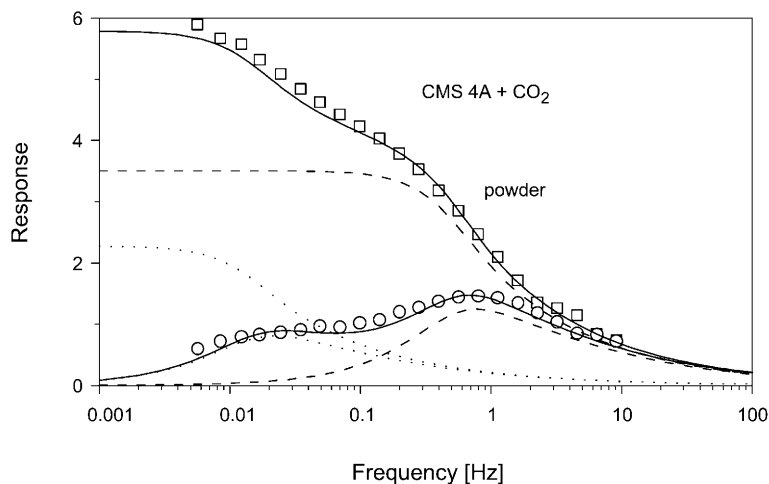


Fig. 2. FR Spectra of CO_2 sorption measured in CMS 4A powder (ca. 500 mg sample) at 133 Pa and -20°

controlling mechanism (Figs. 1 and 2). On grinding, the rate-determining step changes from intercrystalline-diffusion to parallel intracrystalline-diffusion processes. CO_2 , having the smallest kinetic diameter among the applied gas probes, is the most sensitive in probing the slit-like carbon micropores.

Upon comminution of the carbon pellets probing with N_2 (Fig. 3), the same mechanism change can be observed as with CO_2 . Because the N_2 coverage was low and the FR signals were weak at -20° , the FR measurements were carried out at lower temperature (-78°). On the base of the findings shown in Fig. 3, it can be definitely concluded that the intercrystalline-diffusion resistance can be completely removed by using CMS 4A adsorbent particles smaller than 1 mm diameter. It is surprising that further grinding has no significant influence on the FR spectra. This behavior is quite different from that compared to the ground zeolite beads. Additional N_2 spectra on three other carbon samples are measured for comparison. The spectra of a commercial activated-carbon (AC) sample show the same invariance in the function of the particle size (Fig. 3). The resonance signal on the rate spectrum at N_2 adsorption appears at much higher frequencies reflecting much smaller diffusion-time constants, less intracrystalline-diffusion resistances, and suggesting wider micropores. The last finding is confirmed by the change in the shape of the responses, *i.e.*, a transition can be observed in the rate-controlling process from intracrystalline diffusion to the adsorption/desorption step (see the intersections of component curves). (If sorption is the lowest, one of the consecutive steps of mass transport, according the theory of the

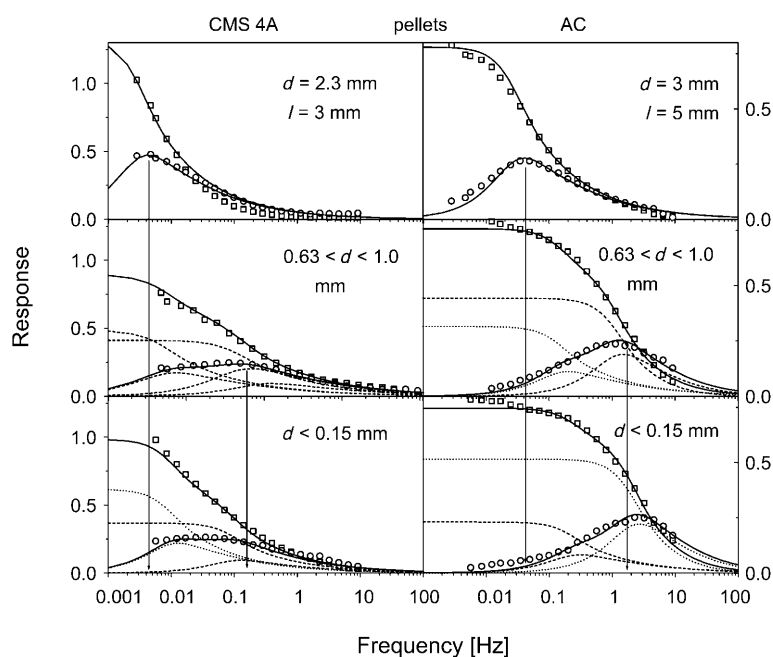


Fig. 3. FR Spectra of N_2 sorption recorded in different particle fractions of commercial Takeda CMS 4A and Chemviron activated carbon (AC) (ca. 200 mg samples) at 133 Pa and -78°

FR method, the FR component curves intersect at the maximum of the out-of-phase peak and half height of the step-like in-phase curve.)

N_2 Spectra were measured also on charcoal cubes prepared from spruce wood in our lab (Fig. 4). The carbonized spruce-wood cubes (CMS cubes) were faster in adsorbing N_2 than the extruded commercial CMS 4A. Because of the negligible macropore diffusion resistance, the difference in the resonance frequencies determined for the large (8 mm) carbon cubes and their powder is small. The sorption properties of the commercial carbon pellets have much stronger response to comminution. The spectra of the different-size fractions seem to be identical and characteristic for mass transport in micropores (Fig. 4). CMS Cubes containing narrower micropores proved to be a more effective carbon molecular sieve for air separation compared to commercial CMS 4A characterized with kinetic-selectivity values ($S_k = t_{N_2}/t_{O_2}$) 14 and 3, respectively [15]. The sorption process is almost completely rate-controlled by the slow intracrystalline diffusion. In the activated carbonized wood cubes (AC cubes), a very fast ad/desorption process is detected as rate-determining step, not influenced by diffusion resistance. The response signal appears near to the upper experimental frequency limit. The increased size of carbon cube is of a weak influence on the time constant.

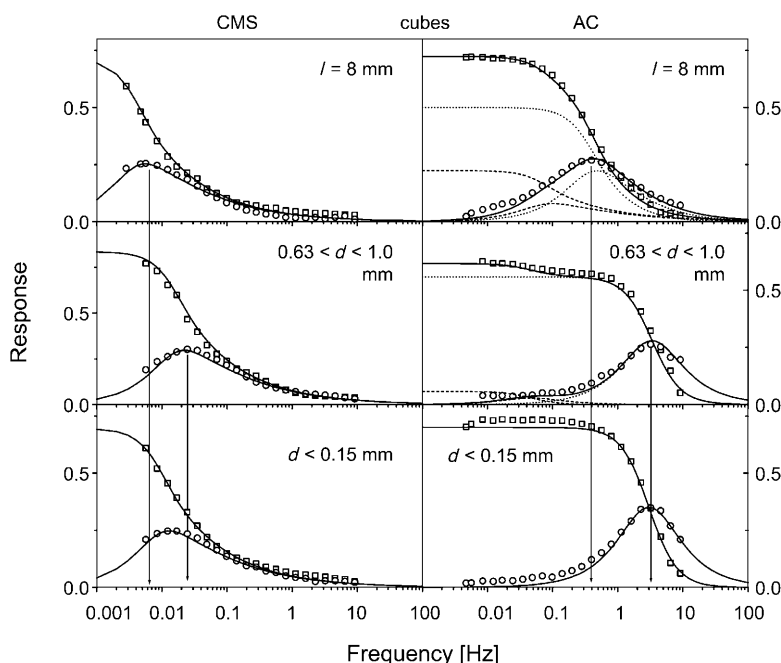


Fig. 4. FR Spectra of N_2 on carbonized-spruce wood cubes (CMS cubes) or after deep oxidative activation (AC cubes) (ca. 200 mg samples) at 133 Pa and -78°

The molecular mobility in carbon adsorbents is basically determined by the adsorbent texture. SEM Images reveal the structural differences of commercial- and laboratory-carbon preparations (Fig. 5). The pelletized CMS 4A does not show an ordered pore structure at this magnification (Fig. 5,a). The commercial CMS

adsorbents are often produced by pelletization of powdered activated carbon. Their macropore structure and hereby the overall diffusion resistance are strongly dependent on the type of raw material and the pelletization technique of the activated-carbon powder. The carbonization of spruce-wood cubes resulted in an excellent carbon honeycomb structure, which is formed from the vascular walls of channels of the spruce-wood log (*Fig. 5, c*). The diameter of the channels is *ca.* 20–30 μm , offering fast gas transport with low diffusion resistance. The *ca.* 3 μm thick walls contain easily accessible microporous graphitic crystals having a high adsorption capacity. This type of macroporosity seems to be ideal from a dynamic point of view for applications in short-cycle adsorption-separation technologies. In the SEM image of the commercial activated carbon (*Fig. 5, b*), structural fragments can be seen which seem to be similar to the carbon skeleton of the spruce cube. The small fragments of CMS 4A can not be recognized at the applied magnification; however, the results show that, after comminution below 1 mm, the micropores of carbons become fully accessible through macropores stemming from the preserved biological structure of the carbonized plants.

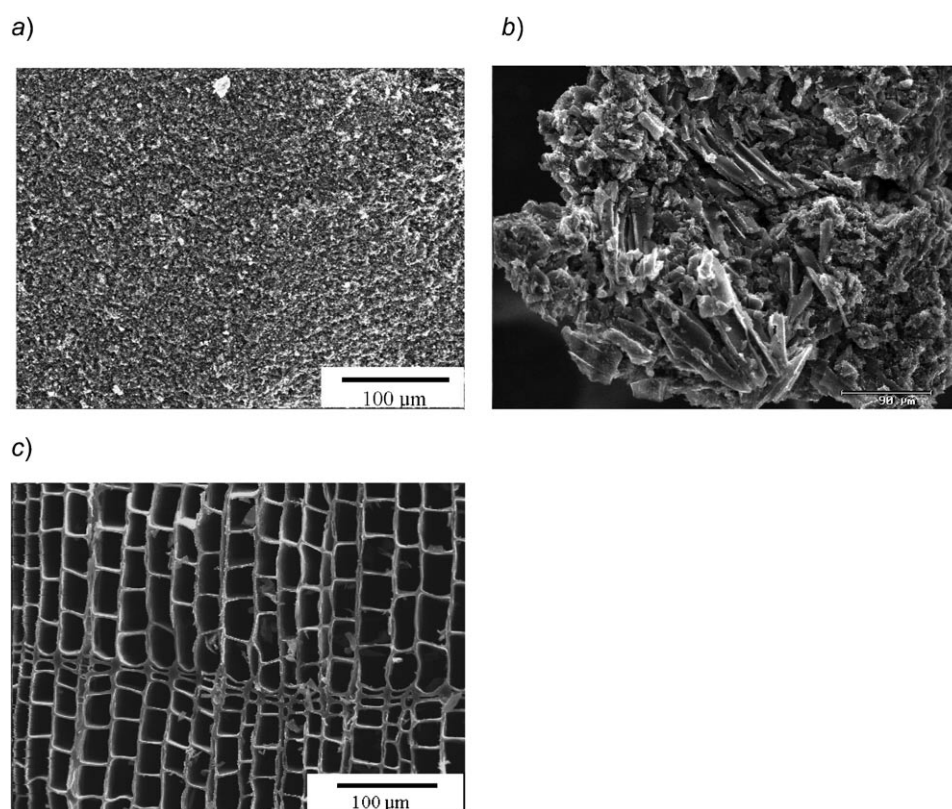


Fig. 5. Scanning-electron-micrograph (SEM) images of a) the Takeda CMS 4A, b) the commercial activated-carbon pellet (Chemviron), and c) the carbonized spruce cube, respectively

Zeolite 4A could not be investigated with the FR technique because of the extremely low micropore diffusivities. Thus, zeolite 5A having the same framework as zeolite 4A was studied. Adsorption isotherms are compared in *Fig. 6*. Measurements were carried out in the 0–100 kPa range. More data points were obtained at pressures where the isotherms obey *Henry's law*. Thus, the adsorption equilibrium constants (K) could be obtained as the slope of isotherms in the linear low-pressure range. The thermodynamic-selectivity coefficients ($\alpha = K_1/K_2$) were calculated for pairs of adsorptive gases as given in *Table 2*. The FR measurements were carried out in the *Henry region*.

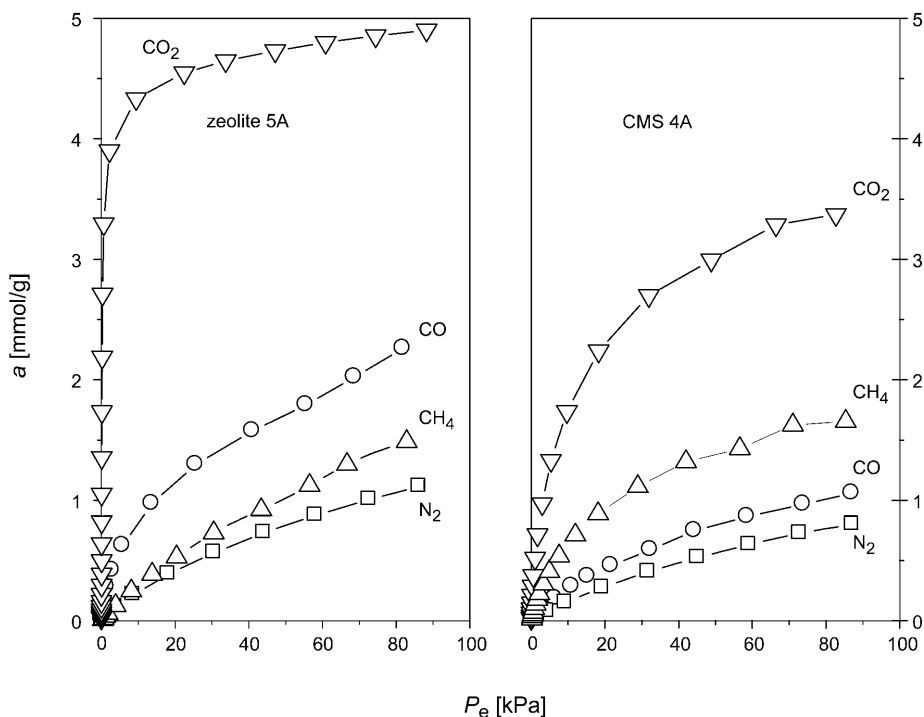


Fig. 6. Isotherms of gas adsorption at -20° for samples treated overnight in a dry N_2 flow at 350°

Table 2. Henry Constants K [$\text{mmol g}^{-1} \text{kPa}^{-1}$] and the Thermodynamic-Selectivity Coefficients (α) Determined at -20°

	K_{CO_2}	K_{CO}	$K_{\text{CO}_2}/K_{\text{CO}}$	K_{CH_4}	$K_{\text{CO}_2}/K_{\text{CH}_4}$	K_{N_2}	$K_{\text{CO}_2}/K_{\text{N}_2}$
Zeolite 5A	12.8	0.33	37	0.035	353	0.037	334
CMS 4A	0.92	0.035	26	0.126	8	0.019	48

It is not surprising that the zeolite structure containing metal cations in high density and the carbon having O-containing functional groups on nonpolar pore walls show very different adsorption capacities and selectivities. At the much higher pressure of an industrial gas-separation process, the competitive adsorption of the gas components

strongly affects separation efficiency. However, the *Henry* constants and the selectivity coefficients give orientation in selecting the right adsorbent to solve a particular gas-separation problem.

The dynamic sorption properties of adsorbents can be evaluated on the basis of the FR spectra. Their FR characteristics recorded for zeolite 5A beads and its powdered form are shown in *Fig. 7*. The dynamic adsorption properties of the zeolite 5A beads were similar to those of zeolite 13X or CMS 4A (*Fig. 1*). Regarding the diffusion in the intercrystalline macro- and mesopores, the structural differences of the zeolites LTA (5A) or FAU (13X) appear only for adsorptives CO and CO₂. The strong interaction between the gas molecules and the pore walls results in slower macropore diffusion. In Ca,Na-A (*i.e.*, 5A) zeolite in contrast to Na-A (4A), the eight-ring apertures are free, resulting in faster diffusion than in the zeolite 4A. However, the CO₂ FR spectrum of zeolite 5A beads can not yet be observed in the available frequency window.

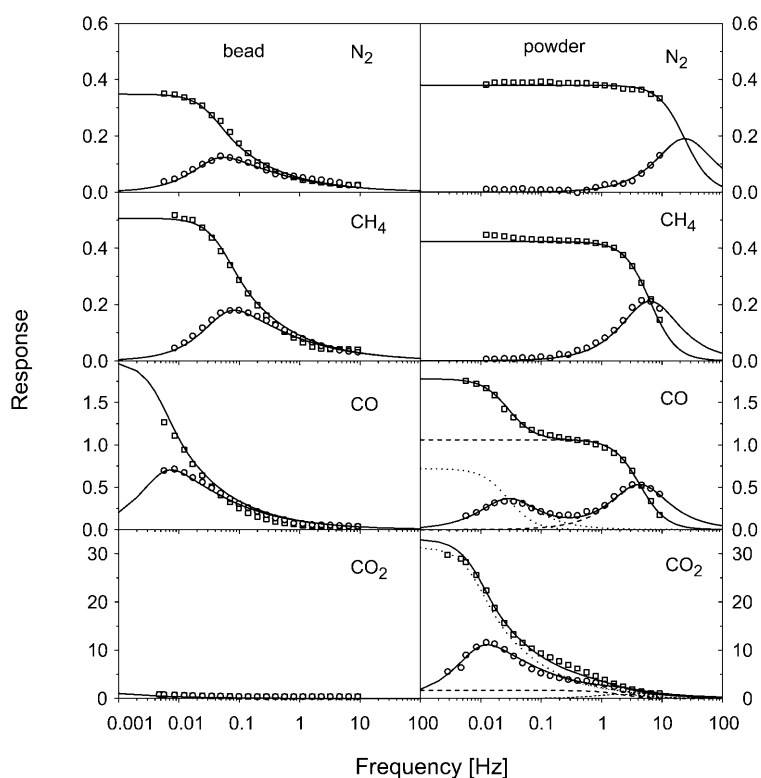


Fig. 7. FR Spectra of N₂, CH₄, CO, and CO₂ obtained in 5A beads and powder (ca. 500 mg samples) at 133 Pa and –20°

The diffusion resistance of the macropores can be removed by comminution of the adsorbent pellet. In the powdered zeolite 5A, the rate of the intracrystalline diffusion (CO₂) or adsorption/desorption step (N₂, CH₄, CO) governs the rate of mass transport (*Fig. 7*). The FR spectrum of CO showed two distinct resonance signals demonstrating

the transition of the rate-controlling mechanism from sorption to intracrystalline diffusion.

FR Spectra of CO₂ on powdered zeolite 5A were recorded at additional different temperatures (*Fig. 8*). Upon decreasing the temperature or increasing the coverage of the sorption sites, the rate-controlling step of mass transport changes from sorption to intracrystalline diffusion. A similar behavior was observed for zeolite 13X. These results demonstrate that the mechanism of sorption mass transport can depend on temperature and the extent of micropore filling.

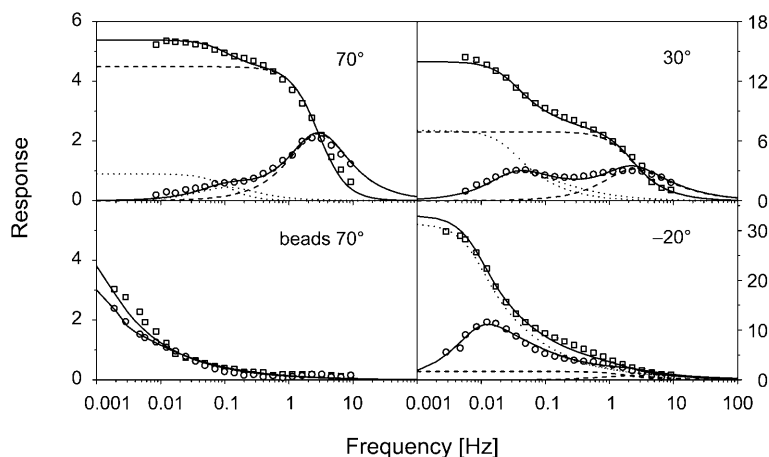


Fig. 8. FR Spectra of CO₂ sorption in 5A beads (ca. 500 mg sample) at 70° and powders at different temperatures at 133 Pa

The sorption capacities of CMS 4A are about the same for N₂ and CO, having similar molecular mass and size ($K_{\text{CO}}/K_{\text{N}_2} = 1.8$). Also these molecules have similar characteristic times of diffusion (see *Table 3*, $D_{\text{N}_2}/D_{\text{CO}} = 1.6$). The zeolite 5A adsorbents represent a different case. Data suggest that the zeolites are more effective in the sorption separation of these gases than the carbon ($K_{\text{CO}}/K_{\text{N}_2} = 8.9$ and $D_{\text{N}_2}/D_{\text{CO}} = 7.6$). In contrast, N₂ and CH₄ diffusion in zeolites have similar characteristic times, while the carbon adsorbent can be kinetically effective in separating these gases ($D_{\text{N}_2}/D_{\text{CH}_4} =$

Table 3. Characteristic Times of Intercrystalline Diffusion and Macropore Diffusivities Determined at –20°

	t_{CO_2} [s]	t_{CO} [s]	t_{CH_4} [s]	t_{N_2} [s]
Zeolite 5A	< 1000	220	22	29
Zeolite 13X	< 1000	130	20	24
CMS 4A	330	32	200	20
	D_{CO_2} [m ² /s]	D_{CO} [m ² /s]	D_{CH_4} [m ² /s]	D_{N_2} [m ² /s]
Zeolite 5A	$> 1.1 \cdot 10^9$	$5.0 \cdot 10^9$	$50.0 \cdot 10^9$	$38 \cdot 10^9$
Zeolite 13X	$> 1.1 \cdot 10^9$	$8.5 \cdot 10^9$	$55.0 \cdot 10^9$	$46 \cdot 10^9$
CMS 4A	$3.3 \cdot 10^9$	$34.0 \cdot 10^9$	$5.5 \cdot 10^9$	$55 \cdot 10^9$

10, see Table 3). However, the thermodynamic selectivity is inverse ($K_{\text{CH}_4}/K_{\text{N}_2} = 6.6$). On the bases of diffusional-time constants or rather macropore transport diffusivities, zeolites seem to be more advantageous for a kinetic separation of CO_2 and CH_4 than CMS 4A. In the case of the CO_2 and CO pair adsorbed on the zeolite, 13X has a nice kinetic-separation factor ($D_{\text{CO}}/D_{\text{CO}_2} = 7.7$); however, the carbon is characterized by short characteristic times, *i.e.*, fast diffusivities, which, together with a good separation factor ($D_{\text{CO}}/D_{\text{CO}_2} = 10$), is a double advantage in a short-cycle adsorption technology. The use of both experimental equilibrium and kinetic selectivities in the practice seems to be complicated because the effects can be reverse.

The research described in this article was supported by the *National Office for Research and Technology* (GVOP-3.2.1.-20004-04-0277/3.0) which supports are gratefully acknowledged. The author wishes to express his appreciation to Dr. *Katalin Papp* for taking the SEM images and Mrs. *Ágnes Wellisch* for her excellent technical assistance.

REFERENCES

- [1] R. T. Yang, 'Adsorbents: Fundamentals and Applications', John Wiley & Sons, Hoboken, New Jersey, USA, 2003.
- [2] G. V. Baron, in 'E. F. Vansant, Separation Technology', Elsevier, Amsterdam, 1989, p. 201.
- [3] G. Onyestyák, J. Valyon, L. V. C. Rees, in 'Fundamentals of Adsorption 7', Eds. K. Kaneko, H. Kanoh, and Y. Hanzawa, IK International, Ltd., Chiba-City, 2002, p. 755.
- [4] J. Valyon, G. F. Lónyi, Onyestyák, J. Papp, *Microporous Mesoporous Mater.* **2003**, *61*, 147.
- [5] H. Yang, Z. Xu, M. Fan, R. Gupta, R. B. Slimane, A. E. Bland, I. Wright, *J. Environ. Sci.* **2008**, *20*, 14.
- [6] S. Cavenati, C. A. Grande, A. E. Rodrigues, *Chem. Eng. Sci.* **2006**, *61*, 3893.
- [7] N. N. Dutta, G. S. Patil, *Gas Sep. Purif.* **1995**, *9*, 277.
- [8] F. Rezaei, P. Webley, *Sep. Purif. Technol.* **2010**, *70*, 243.
- [9] G. Onyestyák, L. V. C. Rees, *J. Phys. Chem. B* **1999**, *103*, 7469.
- [10] G. Onyestyák, L. V. C. Rees, K. László, *Helv. Chim. Acta* **2004**, *87*, 1888.
- [11] L. V. C. Rees, D. Shen, *Gas Sep. Purif.* **1993**, *7*, 83.
- [12] Y. Yasuda, *Heterogen. Chem. Rev.* **1994**, *1*, 103.
- [13] R. G. Jordi, D. D. Do, *Chem. Eng. Sci.* **1993**, *48*, 1103.
- [14] G. Onyestyák, J. Valyon, A. Bóta, L. V. C. Rees, *Helv. Chim. Acta* **2002**, *85*, 2463.
- [15] G. Onyestyák, Z. Ötvös, K. Papp, *Micropor. Mesoporous Mater.* **2008**, *110*, 86.

Received May 21, 2010